Universiteit
Leiden
The Netherlands

Nucleosome dynamics resolved with single-pair fluorescence resonance energy transfer spectroscopy

Koopmans, W.J.A.

Citation

Koopmans, W. J. A. (2009, June 18). *Nucleosome dynamics resolved with single-pair fluorescence resonance energy transfer spectroscopy*. Retrieved from https://hdl.handle.net/1887/13856

Version:	Corrected Publisher's Version
License:	Licence agreement concerning inclusion of doctoral thesis in the Institutional Repository of the University of Leiden
Downloaded from:	https://hdl.handle.net/1887/13856

Note: To cite this publication please use the final published version (if applicable).

Chapter 4

Nucleosome Immobilization Strategies for Single-Pair FRET Microscopy[1]

Abstract All genomic transactions in eukaryotes take place in the context of the nucleosome, the basic unit of chromatin, which is responsible for DNA compaction. Overcoming the steric hindrance that nucleosomes present for DNA-processing enzymes requires significant conformational changes. The dynamics of these have been hard to resolve. Single-pair Fluorescence Resonance Energy Transfer (spFRET) microscopy is a powerful technique for observing conformational dynamics of the nucleosome. Nucleosome immobilization allows the extension of observation times to a limit set only by photobleaching, and thus opens the possibility of studying processes occurring on timescales ranging from milliseconds to minutes. It is crucial however, that immobilization itself does not introduce artifacts in the dynamics. Here we report on various nucleosome immobilization strategies, such as single point attachment to polyethylene glycol (PEG) or bovine serum albumin (BSA) coated surfaces, and confinement in porous agarose or polyacrylamide gels. We compared the immobilization specificity and structural integrity of immobilized nucleosomes. A crosslinked star polyethylene glycol coating performed best with respect to tethering specificity and nucleosome integrity, and enabled us for the first time to reproduce bulk nucleosome unwrapping kinetics in single nucleosomes without immobilization artifacts.

[1]This chapter is based on: W. J. A. Koopmans, T. Schmidt, and J. van Noort, Nucleosome Immobilization Strategies for Single-Pair FRET Microscopy. *ChemPhysChem* **9**, 2002-2008 (2008)

4.1 Introduction

Nucleosomes form the basic unit of DNA organization in eukaryotic nuclei. A nucleosome core particle comprises 147 base pairs (bp) of DNA wrapped 1.7 turns around a histone octamer protein core [1]. This tight compaction makes most of the nucleosomal DNA inaccessible to proteins involved in processes such as transcription, replication, and repair. However, several pathways that provide accessibility to nucleosomal DNA [2] have been identified, including transient DNA unwrapping [3], thermal and ATP-driven enzymatic nucleosome repositioning [4], and histone exchange [5]. These processes occur on various time scales, ranging from milliseconds for DNA unwrapping to minutes or hours for thermal nucleosome repositioning. Single-pair Fluorescence (or Förster) Resonance Energy Transfer [6] (spFRET) microscopy has the potential to reveal these mechanisms in individual nucleosomes with unprecedented detail, since it is sensitive to conformational changes of 2-10 nm. In recent spFRET experiments on nucleosomes, energy transfer was detected from short bursts of fluorescence as single nucleosomes diffused through a small confocal detection volume [7–9]. Since the average diffusion time was on the order of 1 ms, it was not possible to resolve slow (>10 ms) conformational dynamics with this approach, limiting the applications to only a small subset of the anticipated conformational changes. Sample immobilization can provide the extended observation time needed for directly observing slow dynamics as demonstrated by two spFRET studies on nucleosomes tethered to a surface. Tomschik *et al.* placed a FRET pair far inside the nucleosome, thereby targeting major disruptions of nucleosomal structure [10]. However, reevaluation of their data led to the conclusion that the observed FRET dynamics was dominated by photoblinking of the dyes [11]. In a slightly different approach, we performed spFRET microscopy, under conditions that suppressed blinking, on immobilized mononucleosomes that were labeled at the dyad axis and the nucleosome exit [12]. We observed DNA unwrapping dynamics in only 3% of the nucleosomes. We found however that the vast majority of nucleosomes was disrupted, resulting in an absence of FRET. Furthermore, the observed kinetics were much slower than anticipated based on bulk experiments by Li *et al.* [13] From these effects we concluded that both nucleosome structure and DNA breathing dynamics were influenced by immobilization of nucleosomes to the surface. In this study we explore a number of immobilization strategies that were successful in other single-molecule assays for their ability to reduce surface artifacts. The physical properties of nucleosomes require a tailored solution to provide an inert local environment. The high level of bending of the nucleosomal DNA effectively renders the nucleosome to be a loaded spring [14]. Nucleosomes rapidly dissociate to form sub-stoichiometric DNA-histone complexes [15, 16] at the 10-100 pM concentrations needed for single-molecule detection. Furthermore, the pronounced charge distribution on the nucleosome surface, with negatively charged DNA bound to positively charged

histones, makes the nucleosome a highly salt-sensitive structure [17]. Finally, histone proteins are known to stick to many types of glass and plastic surfaces [18]. Thus, nucleosomes provide a magnificent challenge to be immobilized such, that they don't interact non-specifically with the surface, and that they retain their canonical structure. In single-molecule fluorescence microscopy several immobilization schemes have been employed successfully (reviewed by Rasnik [19]), such as specific tethering to BSA-biotin [20] or polyethylene glycol (PEG) [21] coated surfaces, encapsulation in lipid vesicles [22], and immobilization in the aqueous pores of polyacrylamide (PA) [23] or agarose gels [24]. Although each immobilization scheme has its own merits, a universal strategy does not exist: for example, BSA surface coatings were too adhesive for studies involving Rep helicase protein [21] but PEG coated surfaces provided a good alternative. In a different study however, it was shown that RNaseH denatured when immobilized to PEG coated surfaces [25]. Thus, each DNA-protein complex requires a tailored immobilization strategy for single-molecule fluorescence microscopy studies. In order to find an optimal strategy for immobilizing complex multi-subunit DNA-protein assemblies like the nucleosome, we systematically tested several immobilization procedures on fluorescently labeled nucleosomes: immobilization in PA and agarose gels, and specific tethering to BSA-biotin or PEG coated surfaces. We used total internal reflection fluorescence (TIRF) microscopy and alternating excitation [26] (ALEX) to identify donor- and acceptor-only species, and to resolve bleaching and blinking events. Both gel immobilization procedures resulted in unacceptable signal-to-noise ratios (SNR). We subsequently characterized surfaces for their resistance to non-specific binding of nucleosomes, and the effect of the surface on nucleosome structural integrity, as judged by the FRET efficiency of individual nucleosomes. A crosslinked star PEG coating [27] performed best with respect to tethering specificity and nucleosome integrity, and enabled us to reproduce the nucleosome unwrapping kinetics determined by Li *et al.* [13] using bulk fluorescence methods, in single nucleosomes.

4.2 Results and Discussion

Mononucleosomes were prepared on a fluorescently labeled, biotinylated DNA construct as schematically shown in figure 4.1. As determined by absorption measurements, the labeling efficiency of the primer DNA was 70% for the acceptor and 90% for the donor, despite HPLC purification after primer synthesis. Upon reconstitution with stoichiometric amounts of histone proteins, the 601 nucleosome positioning sequence [28] places the donor and acceptor at the nucleosome dyad axis and exit respectively. The average FRET efficiency of the nucleosome sample in solution was 0.3, as determined by bulk fluorescence measurements (figure 4.1.b). In previous single molecule experiments we measured the FRET efficiency of single nucleosomes with dyes at the same locations to be 0.6. Accordingly, taking incomplete labeling

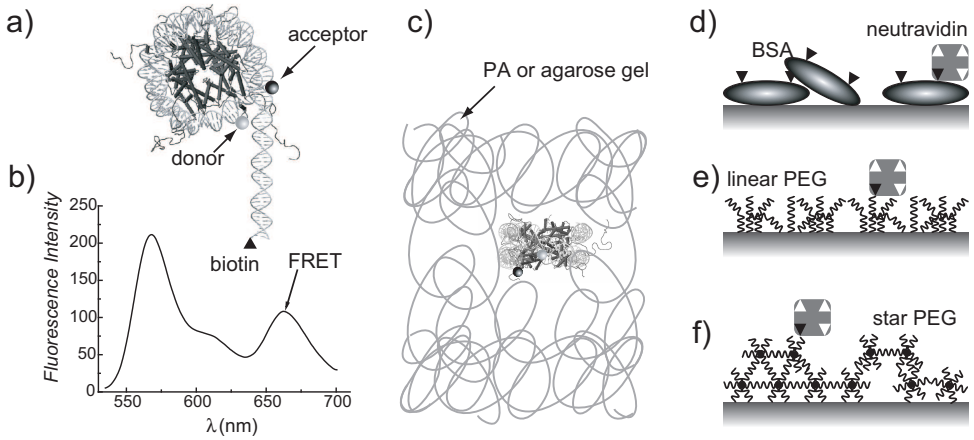

Figure 4.1: Overview of the tested nucleosome immobilization strategies. a) Schematic of the nucleosome construct. The label positions of donor and acceptor are indicated with circles, a biotin modification at the DNA end is indicated with a triangle. b) Bulk fluorescence spectrum of reconstituted nucleosomes. The distinct acceptor emission peak is indicative of reconstituted nucleosomes. c) Gel immobilization, by trapping nucleosomes in the aqueous pores of a polyacrylamide or agarose gel matrix. d)-f) Surface immobilization, by tethering nucleosomes to a glass slide with (d) a BSA-biotin coating, (e) a linear PEG coating, or (f) a crosslinked star PEG coating, through biotin-neutravidin-biotin linkage.

of the primers into account, 33% of the DNA molecules were properly reconstituted into nucleosomes and showed efficient FRET, while another 33% was doubly-labeled free DNA. Thus, when nucleosome integrity is not affected by immobilization we expect a maximum yield of nucleosomes with efficient spFRET of 33%. We tested five nucleosome immobilization strategies, as illustrated in figure 4.1. First, we studied confinement in the aqueous pores of (i) PA gel or (ii) agarose gel matrices (figure 4.1.c). Both agarose and polyacrylamide gel electrophoresis are routinely employed to separate and isolate nucleosomes from free DNA. Since nucleosomes migrate in sharp bands and retain their proper folding in native gel electrophoresis assays, we reasoned that agarose and PA gels are relatively inert to nucleosomes. Alternatively, we studied nucleosome tethered to (iii) BSA-biotin coatings (figure 4.1.d), (iv) linear PEG coatings (figure 4.1.e), and (v) crosslinked star PEG coatings (figure 4.1.f), which all have been successfully employed in single-molecule fluorescence experiments[19].

4.2.1 Immobilization through confinement in gels

Polyacrylamide gels In PA, gel formation occurs due to polymerization and crosslinking reactions between monomers. At the conditions chosen, i.e. 8% PA, the average pore diameter was ~8 nm [29], sufficiently small to immobilize the 11x6 nm sized nucleosomes. Indeed, we

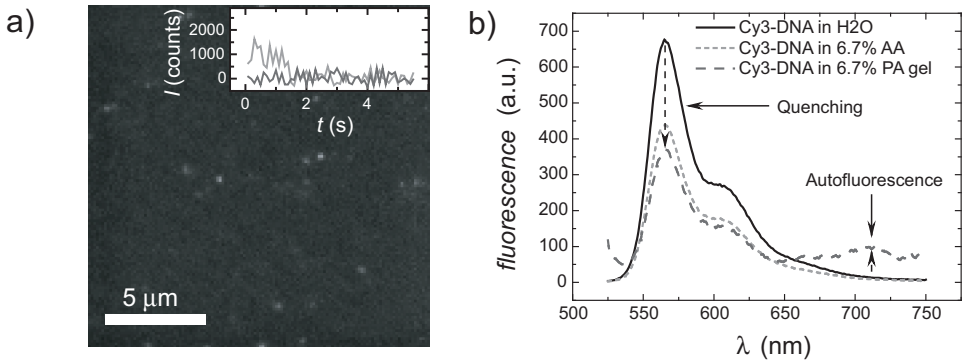

Figure 4.2: Immobilization in PA gels. a) Fluorescence image of 100 pM Cy3-ATTO647N labeled nucleosomes in an 8% PA gel. The fluorescence intensity was reproducibly low, and often either donor or acceptor was already bleached (inset). b) Bulk fluorescence emission spectrum of Cy3-labeled DNA in water, in a 6.7% acrylamide solution, and in a 6.7% PA gel. Fluorescence emission was quenched in acrylamide gels, and autofluorescence was observed at ~700 nm.

observed many immobilized fluorophores, as depicted in figure 4.2.a. We found however that only a small fraction of the molecules was doubly labeled when immobilized in PA. Most of the fluorescence originated from donor-only (45%) or acceptor-only (25%) species, as deduced by alternating excitation (ALEX). Therefore 40% of the donor and 40% of the acceptor were absent in the gel, probably due to bleaching by free radicals that catalyze the polymerization process. Next to the degradation of the dyes, the observed signal intensity from a single fluorophore was low ($0.9 \pm 0.4 \cdot 10^3$ counts), as compared to the background noise of $0.2 \cdot 10^3$ counts, leading to signal-to-noise ratio (SNR) of 2 and signal-to-background ratio (SNB) of 5. In comparison, at similar excitation intensity (0.75 kW/cm^2) and illumination time (40 ms), the intensity of either donor or acceptor from individual nucleosomes immobilized to a coated surface was $2.2 \pm 0.3 \cdot 10^3$ counts, resulting in a SNR and SNB of 8 and 11, respectively. The reason for the low SNR and SNB in single-molecule experiments was inferred from bulk fluorescence experiments on Cy3-labeled DNA oligomers immobilized in 6.7% PA (figure 4.2.b). We found a 30% decrease of fluorescence intensity for Cy3 in 6.7% acrylamide (AA), which is a known fluorescence quencher [30]. Upon polymerization into PA, the fluorescence intensity dropped an additional 20%. Furthermore a broad band of autofluorescence around 700 nm emerged. This autofluorescence was also observed in gels without immobilized fluorophores, and should therefore be attributed to the PA gel itself. In conclusion, we observed an increase in donor-only and acceptor-only species, a decrease in fluorescence intensity and a low SNR and SNB due to a combination of bleaching by free radicals, quenching by unpolymerized AA

and background autofluorescence from the PA gel. How does this compare to previous studies using the same methodology? We did not obtain a high SNR as obtained by Dickson *et al.* for Nile red in a 18% PA gel [23] or GFP in a 15% PA gel [31]. However, nile red probably showed an acceptable SNR because of its high quantum yield (0.7), in combination with the high excitation intensity (5 kW/cm^2) and long exposure time (100 ms) used by Dickson *et al.* Due to rapid photobleaching under these illumination conditions, the observation time was limited to ~10 data points however. In the case of GFP, bleaching by free radicals or quenching by unpolymerized AA is unlikely to occur, because the fluorophore is protected by a protein barrel. In summary, nucleosome immobilization in PA gels is not productive because of the low SNR and the loss of doubly labeled molecules.

Agarose Gels Alternatively, we immobilized nucleosomes in 3% agarose gels [24]. Unlike polymer gels like PA, where gel formation occurs by chemical polymerization and crosslinking reactions between monomers, agarose forms a physical gel upon cooling below the gelling temperature (~35 °C for low melting agarose). Furthermore, agarose is not known to quench fluorescence. Using epifluorescence we imaged number of immobilized nucleosomes in the agarose gel. The SNR (~3) and SNB (~4) were poor however compared to TIRF imaging, and did not improve with longer exposure times. We attribute this to out-of-focus fluorescence emission from nucleosomes in the agarose gel, and from the buffer layer, where freely diffusing nucleosomes accumulated. Using TIRF, we observed that the agarose gel did not adhere to the cover slide, resulting in a 1-2 µm layer of buffer between the glass and the agarose gel. Nucleosomes could freely diffuse in this layer. This gap was always present, even when we prepared the agarose film using spincoating, or with thin intermediate coatings such as methylcellulose, poly-D-lysine, or sigmacote (Sigma). TIRF imaging of immobilized nucleosomes in the gel was therefore not possible, since the evanescent excitation field only extended a few 100 nm into the buffer. On top of the accumulation of free nucleosomes between the gel and the surface we did not achieve sufficient protein immobilization in agarose gels to allow for extended imaging times using epifluorescence, unlike Lu *et al.* [24]. Immobilization by confinement alone however is unlikely in a 1% gel with an average pore diameter of ~140 nm, as noticed by Gai et al, who also reported a buffer layer between the gel and the cover slide [32]. Kelbauskas *et al.* confirmed, using FCS, that nucleosomes embedded in a 3% agarose gel show reduced diffusion only by a factor of 10-100 slower [9]. In conclusion, for various reasons gel immobilization did not work for studying long term dynamics of nucleosomes, and alternative immobilization strategies, such as immobilization to a surface, are needed.

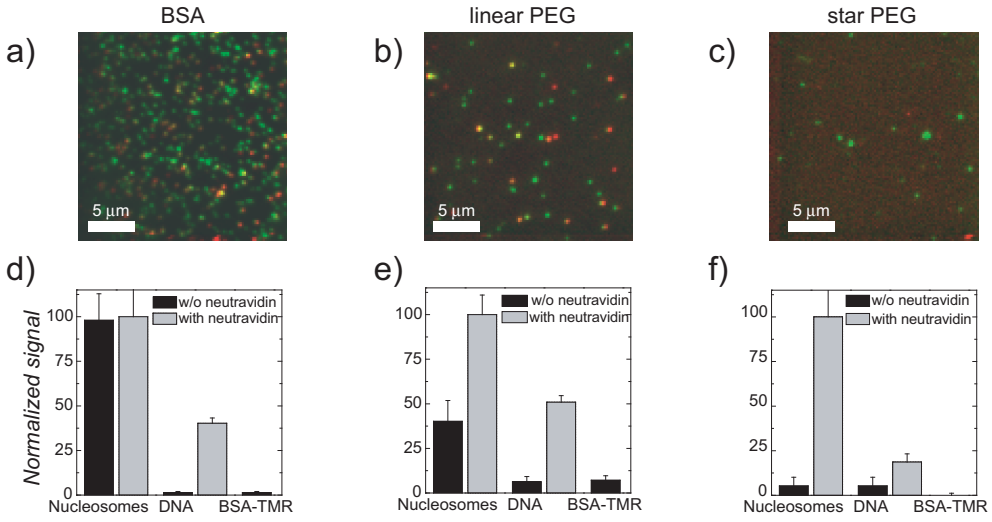

Figure 4.3: Nucleosome binding specificity. Fluorescence image of 100 pM Cy3-ATTO647N labeled nucleosomes bound non-specifically to BSA (a), linear PEG (b), or star PEG (c) coated cover slides, when neutravidin incubation was omitted. Non-specific binding was quantified through a comparison with the amount of fluorescent spots when the same concentration of nucleosomes was bound to BSA (d), linear PEG (e), or star PEG (f) coated slides after incubation with neutravidin. Non-specific binding of 100 pM Cy3-ATTO647N labeled DNA or 100 pM BSA-TMR was negligible on all surface coatings.

4.2.2 Surface immobilization: binding specificity

We immobilized biotinylated nucleosomes to BSA, linear PEG, or star PEG treated glass cover slides through biotin-neutravidin-biotin attachment. We exposed these surfaces to 100 pM fluorescently labeled nucleosomes, and imaged the fluorescence. The specificity of immobilization was tested by quantification of non-specific adhesion of nucleosomes to surfaces prepared without neutravidin. The resulting single- molecule fluorescence images are shown in figure 4.3.a-c. The large number of fluorescent spots shows that nucleosomes readily adhere to BSA-coated glass (figure 4.3.a). The linear PEG coating prevented non-specific adsorption to some extent (figure 4.3.b). Star PEG coatings however were superior, and showed negligible nucleosome binding when the neutravidin incubation was omitted (figure 4.3.c). We quantified the amount of non-specific adhesion by counting the number of fluorescent spots in each image (figure 4.3.d-f), and normalized this to the amount of binding observed on surfaces which were incubated with neutravidin. For BSA we found no significant difference between neutravidin treated and untreated surfaces. For linear PEG coatings we found that ~40% of the molecules were immobilized non-specifically, while for star PEG coatings this was less than 10%. We repeated these experiments for neutravidin treated surfaces with non-biotinylated nucleosomes, to test whether nucleosomes interacted non-specifically with the neutravidin. The same trend was observed: nucleosomes showed significant binding to the BSA (~1 /μm²), limited binding to the linear PEG (~0.2 /μm²), and negligible binding to the star PEG (~0.03 /μm²) coated glass. Therefore, non-specific binding should be attributed to the surface rather than to the neutravidin. To resolve nucleosome-specific properties of these surface coatings and to relate these previous reports [19] we tested them for preventing DNA and BSA adsorption (figure 4.3.d-f). Non-specific binding of the DNA construct alone was negligible on all surfaces. None of the surface coatings showed any fluorescence when exposed to fluorescently labeled BSA. Thus, though all tested surfaces prevented non-specific interactions with DNA and BSA-protein, only star PEG coatings provided sufficient resistance to nucleosome adsorption. Since no DNA binding was observed, nucleosome adhesion to bare glass, BSA coatings, and PEG coatings must be mediated through the histone proteins in the octamer core. BSA coatings did not prevent nucleosome adsorption at all: the number of fluorescent spots was comparable to that of nucleosomes on bare glass. It is known that physisorbed BSA coatings are inhomogeneous [25]. It is therefore possible that parts of the glass surface were still exposed, resulting in nucleosome adsorption. BSA itself is negatively charged and could interact with the positively charged histone proteins as well. Interactions with DNA are effectively screened though, presumably through electrostatic repulsion. An excess of BSA was always present in the buffer, which explains why all non-specific interactions with labeled BSA-TMR were blocked. The linear PEG coating showed a strong reduction in non-specific interactions with nucleosomes. The covalently attached PEGs form a ~1 nm thick polymer brush that prevents protein adsorption

to the glass surface. Indeed, fluorescently labeled DNA, BSA and streptavidin (data not shown) did not bind non-specifically to the PEG surface. However, 40% of the nucleosomes were attached non-specifically, pointing at interactions between the histones and the PEG polymers. Although PEG surfaces are inert for many protein interactions, they have been reported to interact strongly with unfolded proteins [19]. The unstructured histone tails that protrude from the nucleosome core are likely to mediate similar interactions. Furthermore, nucleosomes can undergo large conformational fluctuations under the chosen conditions (H2A-H2B dimer exchange, DNA unwrapping), which may transiently expose the histone proteins. This could facilitate hydrophobic interactions between the PEG chain ends and the histone proteins, resulting in persistent non-specific adsorption [25]. Star PEG coatings however showed almost no non-specific binding of nucleosomes. This exceptional blocking of protein adsorption has been demonstrated before with a number of small proteins [27, 33]. Crosslinking of the PEG extremes results in a higher grafting density of the PEG chains, which blocks the underlying glass surface to a greater extent than linear PEG coatings. Furthermore, crosslinking results in an increased layer thickness and a lower density of PEG chain ends, which may result in a more inert surface coating. In summary, the nucleosome binding specificity was poor on BSA, fair on the linear PEG, but excellent on the star PEG coated surfaces.

4.2.3 Surface immobilization: nucleosome integrity

In order to study intrinsic nucleosome conformational fluctuations, it is necessary that nucleosomes maintain their structural integrity when bound to the surface. With the nucleosome labeling strategy described, we could perform spFRET experiments to test whether nucleosomes remained properly folded upon surface immobilization. With the acceptor positioned at the exit point in the nucleosome any conformational change of the nucleosome, be it DNA unwrapping, dimer dissociation or more rigorous mechanisms, will result in a loss of FRET. We used ALEX [26] to distinguish donor- and acceptor-only species from doubly labeled species. For each molecule on the surface we calculated the FRET efficiency E

$$E = \frac{I_A^{514}}{I_A^{514} + I_D^{514}}, \tag{4.1}$$

and the label stoichiometry S

$$S = \frac{I_A^{514} + I_D^{514}}{I_A^{514} + I_D^{514} + I_A^{636}}, \tag{4.2}$$

where I_D^{514} is the donor intensity when excited at 514 nm, and where I_A^{514} and $I_A^{636}$are the acceptor intensities when excited at 514 nm and 636 nm respectively. Properly folded nucleosomes labeled with both donor and acceptor can be identified by having both high E is high

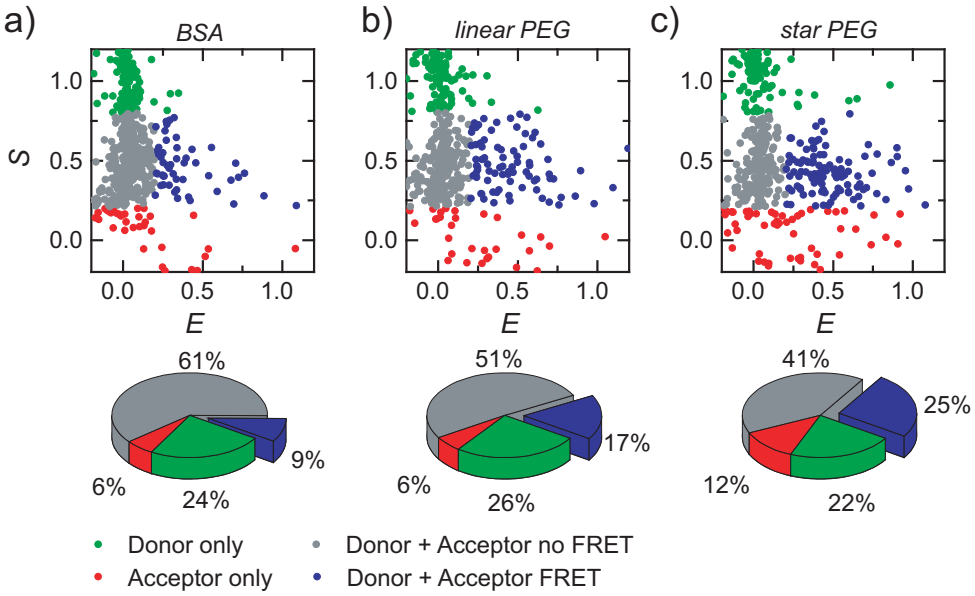

Figure 4.4: Nucleosome structural integrity. 2D scatter plots of the label stoichiometry S versus the FRET efficiency E for nucleosomes bound to BSA (a), linear PEG (b) and star PEG (c) coated cover slides. Each data point represents the average E and S value for a trace until either donor or acceptor bleached. We identified donor-only (S = 1), acceptor-only (S=0) and doubly labeled species (S ~ 0.5). A fraction of the doubly labeled species showed FRET (E > 0.2). This fraction was used as an indicator of nucleosome structural integrity on each surface coating. The relative size of all fractions are summarized in pie-charts (bottom panels)

and S approaching 0.5, assuming comparable quantum yields, absorption cross sections and detector efficiencies for donor and acceptor. The resulting scatter plots of S vs. E for the entire population of nucleosomes are shown in figure 4.4. Each point represents the time averaged E and S value of a fluorescent spot up to either donor or acceptor bleached. We classified fluorescent spots into four categories: canonical nucleosomes with both labels present and showing FRET ($0.2<E<1.2$ and $0.2<S<0.8$); unfolded nucleosomes and bare DNA with both labels present but not showing FRET ($E<0.2$ and $0.2<S<0.8$); donor-only species ($0.8<S$); and acceptor only species ($S<0.2$). The thresholds between the different categories were based on separate measurements (data not shown) of single molecule fluorescence intensity time traces from doubly labeled bare DNA that did not show FRET: from traces where the acceptor bleached first we deduced that $S>0.8$ for donor-only species; from traces where the donor bleached first we deduced that $S<0.2$ for acceptor-only species; from traces before bleaching of either fluorophore, we deduced that $E<0.2$ for bare DNA, since background fluorescence, direct excitation of the acceptor, and crosstalk of donor emission into the acceptor channel never resulted in apparent FRET efficiencies above 0.2 for doubly labeled, bare DNA. On all surfaces the donor-only and acceptor-only populations amounted to ~25% and ~10% respectively, which agreed well with the stoichiometry deduced from bulk absorption measurements on the DNA construct. The population of properly folded nucleosomes, with both labels showing FRET, was 9% for the BSA surface (a), 17% for the linear PEG surface (b) and 25% for the star PEG surface (c), while the population showing no FRET was 61%, 51% and 41% respectively. From the bulk measurements, we estimated that 32% of the molecules were doubly labeled and properly folded. Thus all surfaces featured a destabilization of nucleosomes by the surface. The star PEG surface prevented disassembly of the nucleosomes better than BSA or linear PEG, with 78% of the initial nucleosomes intact. It is known that nucleosomes can be destabilized at low concentrations, presumably due to disassembly of the histone octamer core [15, 16, 34]. This might explain the observed loss in FRET, since the experiments were carried out a low (100 pM) nucleosome concentration in order to get a low enough density of fluorescent spots to resolve individual nucleosomes. However, when the labeled nucleosomes were mixed in a buffer containing 10 nM unlabeled nucleosomes, we found a similar loss in FRET. Consistent with this, we found pronounced differences in nucleosome integrity on the different surface coatings. Thus, surface immobilization, rather than dilution, caused the observed nucleosome disassembly. The linear PEG surface performed better than the BSA coating, but still induced nucleosome destabilization. Conformational changes upon binding to a linear PEG coated surface have been observed before: Heyes *et al.* observed a denaturing of RNaseH when immobilized to a PEG 5000 surface [25]. They attributed this to the flexible PEG chains interacting with the hydrophobic interior of the protein, and/or interactions with the underlying amino functionalized surface. In the case of nucleosomes, these mechanisms

could play a role as well, as demonstrated by the correlation between non-specific adhesion, and a loss of nucleosome integrity. Compared to our previous work [12] using linear PEGs, using star PEGs increased the yield of intact nucleosomes by a factor of 5. The results of our comparison of various nucleosome immobilization strategies are summarized in Table 4.1 on page 62. Since star PEG coatings showed little non-specific binding of nucleosomes and allowed the majority of the nucleosomes to retain their structural integrity, this should put us in a good position to measure nucleosome dynamics without interference of the surface.

Table 4.1: Comparison of various nucleosome immobilization strategies.

Strategy	Immobilization (observation time (s))	SNR	Specificity	Integrity
PA Gel	~1	2	-	-
Agarose Gel	~0.1	3	-	-
BSA-biotin	>10[a]	8	2%	28%
Linear PEG	>10[a]	8	60%	53%
Star PEG	>10[a]	8	90%	78%

[a] limited by photobleaching

4.2.4 Nucleosome breathing dynamics

Spontaneous unwrapping of nucleosomal DNA was previously reported by Li *et al.* [13], who performed FRET based stopped-flow, protein association, and fluorescence correlation spectroscopy experiments on nucleosomes labeled at the histone octamer surface and the DNA exit, probing similar DNA mechanics as in our constructs. From these combined experiments with nucleosomes in solution, on and off times of 250 ms and 10-50 ms respectively could be deduced. Our spFRET experiments allow for direct observation of such DNA breathing in individual nucleosomes, but up to now we could not reproduce the kinetics [12]. To capture all breathing dynamics we performed fast spFRET microscopy (10 ms time resolution) and analyzed the fluorescence intensity traces of nucleosomes immobilized to star PEG coated surfaces. From the traces that showed FRET (25% of the total number of spots), we rejected the traces which had a low SNR (20%), showed photoblinking (5%), uncorrelated intensity changes (10%), or traces with crosstalk from a neighboring FRET pair (8%). In this filtered dataset, we can exclude photoblinking and attributed all FRET dynamics to nucleosome breathing (figure 4.5.a). The FRET efficiency fluctuated reversibly between a high FRET state (E=0.55), originating from a fully wrapped nucleosome, and a distinct low FRET state (E=0.2) originating from an unwrapped state of the nucleosome. A photon and instrument noise analysis [12] enabled us to discriminate between noise and opening events. The lifetime of the closed state was 280 ms, and the lifetime of the open state was 25 ms (figure 4.5.b). These lifetimes are ap-

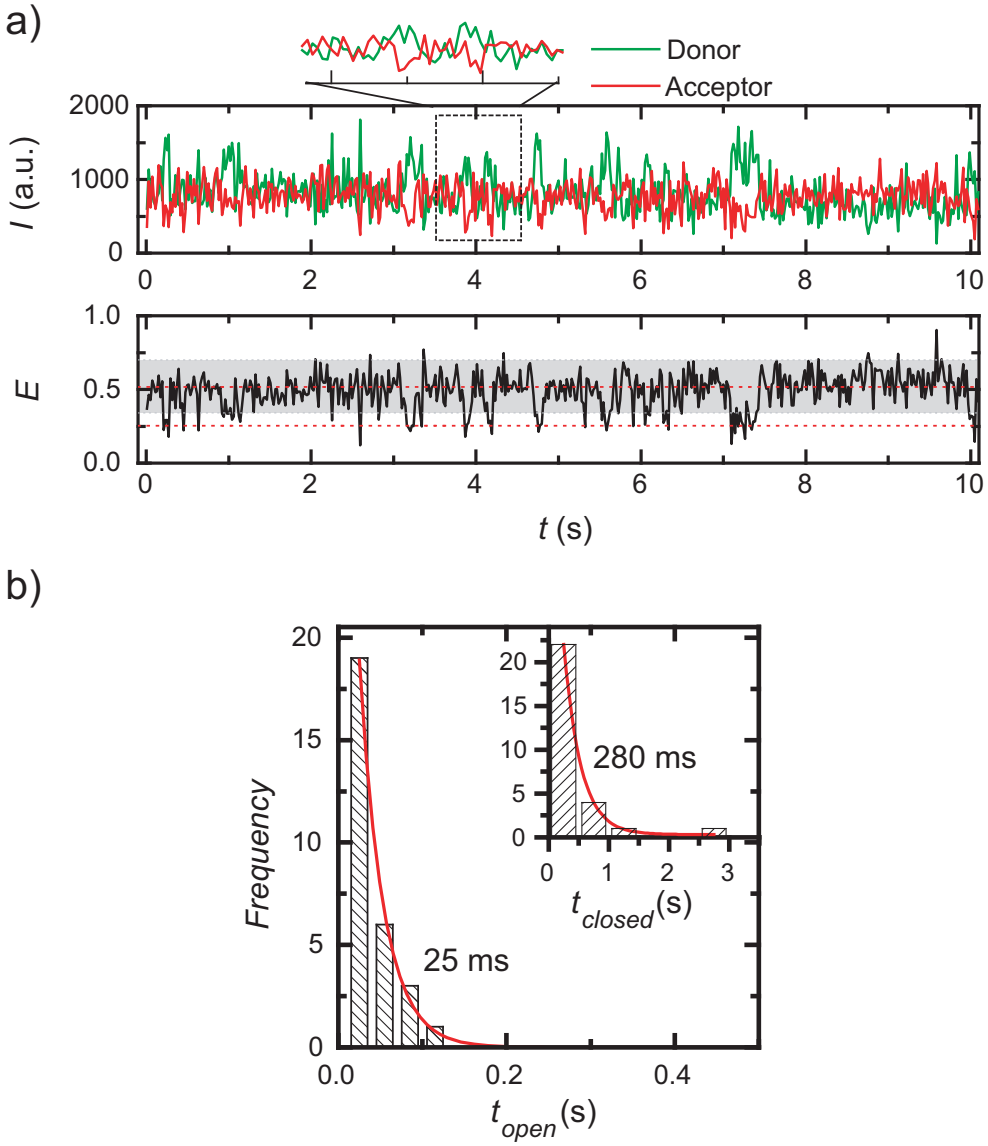

Figure 4.5: Dynamics of nucleosomes immobilized to a star PEG coated surface. a) Fluorescence intensity time trace (top) and corresponding FRET efficiency time trace (bottom). The FRET efficiency fluctuated between a high and a low FRET state, corresponding to a closed and an open nucleosome conformation, respectively. The grey bar indicates a 96% confidence interval for the theoretical photon and instrument noise. b) Histograms of the lifetime of the open and closed (inset) state. The solid lines are exponential fits to the data, yielding lifetimes of 25 ms for the open state and of 280 ms for the closed state.

proximately 5 times faster than the dynamics we observed on linear PEG coated surface (1.5 s closed state, 120 ms open state) but agree perfectly with the nucleosome breathing kinetics of nucleosomes in solution [13]. Thus, nucleosomes can be specifically immobilized on star PEG coatings, while maintaining their structural integrity and their dynamic nature.

4.3 Conclusion

We tested various immobilization strategies for time resolved spFRET microscopy on nucleosomes. Imaging nucleosomes immobilized in polyacrylamide gels was not possible, because of fluorescence quenching, fluorophore bleaching, and autofluorescence. Agarose gels showed limited reduction of diffusion and accumulation of free nucleosomes between the gel and the glass slide, demonstrating the limited applicability of gel immobilization. Surface immobilization allows unlimited observation times but requires a surface tailored to the physical properties of nucleosomes. BSA surfaces were too adhesive, and most nucleosomes disassembled upon immobilization. Linear PEG coatings showed less non-specific adsorption than BSA coatings, but still a large fraction of the nucleosomes disassembled upon immobilization. Crosslinked star PEG coatings however prevented non-specific adsorption and reduced nucleosome disassembly significantly. Using this strategy we were able for the first time to follow DNA breathing dynamics in single nucleosomes yielding the same kinetics as observed for nucleosomes in solution. This opens opportunities to reveal the mechanisms of more complex nucleosomal conformational changes in real time and at the single-molecule level using spFRET. For example assessment of the effect of nucleosome-nucleosome interactions, ATP-dependent remodelers and/or posttranslational modifications on nucleosome stability will provide insight in the physical aspects of gene regulation.

4.4 Experimental Section

Preparation of DNA and nucleosomes Mononucleosomes were reconstituted on a fluorescently labeled 177 basepair (bp) DNA template containing a 601 nucleosome positioning sequence as described [12]. Briefly, the template DNA was prepared by PCR and was labeled with biotin, Cy3 (donor) and ATTO647N (acceptor) by incorporation of fluorescently labeled, HPLC purified primers (IBA GmbH). PCR primers were as follows: forward primer 5'-biotin-TTTGAATTCCCAGGGAATTGGGCGGCCGCCCTGGAGAATCCCGGTGCCGAGGCCGC-3' (acceptor labeled nucleotide is underlined). Reverse primer: 5'-ACAGGATGTATATATCTGACACGTGCCTGGAGACTAGGGAGTAATCCCCTTGGCGGTTAAAACGCGGGGGACAGCGCGTACG-3' (donor labeled nucleotide is underlined. In the DNA template donor and acceptor were located 81 bp (24 nm) apart. Nucleosomes were reconstituted by salt

gradient dialysis with recombinant histones. After reconstitution, donor and acceptor were folded at the dyad axis and nucleosome exit respectively, approximately 4 nm apart, resulting in efficient FRET.

Cover slide preparation Glass cover slides (Assistant, Germany) were sonicated in 1% RBS-50 anionic detergent at 90 °C for 15 minutes, rinsed with milliQ water, sonicated for 1 hour in ethanol (96%), rinsed with milliQ water, dried over a flame, and finally cleaned with a UVO UV ozone cleaning device (Jelight, USA). Slides cleaned in this way showed no detectable residual fluorescence.

Confinement in polymer gels Beaded low melting temperature agarose (BMA, Rockland, ME, USA) was suspended in 1X TE at a 3% w/v ratio. The agarose suspension was melted at 90 °C, and cooled down to 50 °C. Nucleosomes (~100 pM final concentration) were added to the melted gel. The mixture was poured on a cover slide and formed a gel upon cooling to room temperature. In an 8% polyacrylamide gel nucleosomes were immobilized following Dickson *et al.* [23]. Nucleosomes were added to a 8% 29:1 acrylamide:bisacrylamide solution in 1X TE (10 mM Tris.HCl pH 8, 1 mM EDTA), to a final concentration of 100 pM. Polymerization was initiated by adding tetramethylenediamine (0.2% final concentration) and ammonium persulfate (0.05% final concentration). The solution was pipetted on a cover slide, and spread evenly on the slide by covering it with a second slide. Polymerization was complete after 5 minutes.

Surface passivation and functionalization:

BSA coatings Cleaned slides were exposed to biotinylated BSA (0.1 mg/ml, Sigma) for 5 minutes, and rinsed with milliQ water.

Linear PEG Cleaned glass slides were amino functionalized with poly-D-lysine (0.01 mg/ml, Sigma), and subsequently incubated for 4 hours with an amine reactive poly ethylene glycol (PEG) mixture: 20% mPEG-succinimidyl propionate (MW 5 kDa, NOF) and 0.2% biotin-PEG-n-hydroxysuccinimide (MW 3.4 kDa, Nektar Therapeutics) in sodium carbonate buffer (0.1 M, pH 8.2).

Star PEG Six arm NCO PEG stars (MW 12 kDa) were dissolved in tetrahydrofuran (THF) at a concentration of 20 mg/ml, and diluted in milliQ water to a concentration of 2 mg/ ml. Biocytin (Sigma) was added to a final concentration of 1 μg/ml. Five minutes after mixing, the solution was filtered through a 0.22 μm syringe filter (MilliQ), onto the amino functionalized cover slide. When the substrate was fully covered, the slide was spincoated for 45 seconds at

2500 rpm. The slides were incubated at room temperature overnight to complete the crosslinking reaction and were stored in the dark for up to 1 week.

Neutravidin incubation Biotinylated slides were incubated with neutravidin (2 µg/ml, Pierce) for 5 minutes, and were rinsed with milliQ water.

Buffers Experiments were performed in a buffer containing Tris (10 mM, pH 8.0), NaCl (50 mM), and NP-40 (0.03%). For non-specific binding and nucleosome integrity experiments, $MgCl_2$ (2 mM), and BSA (0.1 mg/ml) were added. In some experiments we included unlabeled nucleosomes (10 nM) in the buffer. For nucleosome dynamics measurements, an oxygen scavenger system (glucose oxidase (0.2 mg/ml, Sigma), catalase (0.04 mg/ml, Roche), glucose (4% w/v), and Trolox [35](2 mM)) was added to the buffer, to minimize photobleaching and –blinking.

Single-molecule fluorescence microscopy Single-molecule fluorescence experiments were performed on a setup as described before [12]. Briefly, molecules were imaged on a CCD camera (Cascade 512B, Roper Scientific) through a home-built inverted total internal reflection microscope with an oil immersion objective (100X, 1.45 NA, NIKON). Alternating excitation was achieved by switching between 514 nm and 636 nm laser lines through an AOTF (A.A. Opto-Electronic). Donor and acceptor fluorescence were imaged simultaneously on separate areas of the CCD chip using a dichroic mirror wedge [36].

Acknowledgements

We thank Dr. Jürgen Groll (RWTH Aachen) for providing samples of the NCO-star PEG material and support with the coating procedure, Ineke de Boer and John van Egmond for technical assistance, and Prof. Dr. Alexander Brehm (Philipps-Universtät Marburg) for histone octamer preparations. This work is part of the research programme of the 'Stichting voor Fundamenteel Onderzoek der materie (FOM)', which is financially supported by the 'Nederlandse Organisatie voor Wetenschappelijk Onderzoek (NWO)'.

Bibliography

[1] Luger, K., Mader, A., Richmond, R., Sargent, D., and Richmond, T. Crystal structure of the nucleosome core particle at 2.8 Å resolution. *Nature* **389**, 251–260 (1997).

[2] Luger, K. Dynamic nucleosomes. *Chromosome Res.* **14**, 5–16 (2006).

[3] Li, G. and Widom, J. Nucleosomes facilitate their own invasion. *Nat. Struct. Mol. Biol.* **11**, 763–769 (2004).

[4] Flaus, A. and Owen-Hughes, T. Dynamic properties of nucleosomes during thermal and ATP-driven mobilization. *Mol. Cell. Biol.* **23**, 7767–7779 (2003).

[5] Kimura, H. and Cook, P. Kinetics of core histones in living human cells: Little exchange of H3 and H4 and some rapid exchange of H2B. *J. Cell Biol.* **153**, 1341–1353 (2001).

[6] Ha, T. Single-molecule fluorescence resonance energy transfer. *Methods* **25**, 78–86 (2001).

[7] Gansen, A., Hauger, F., Toth, K., and Langowski, J. Single-pair fluorescence resonance energy transfer of nucleosomes in free diffusion: Optimizing stability and resolution of subpopulations. *Anal. Biochem.* **368**, 193–204 (2007).

[8] Kelbauskas, L., Chan, N., Bash, R., Yodh, J., Woodbury, N., and Lohr, D. Sequence-dependent nucleosome structure and stability variations detected by Förster resonance energy transfer. *Biochemistry* **46**, 2239–2248 (2007).

[9] Kelbauskas, L., Chan, N., Bash, R., DeBartolo, P., Sun, J., Woodbury, N., and Lohr, D. Sequence-dependent variations associated with H2A/H2B depletion of nucleosomes. *Biophys. J.* **94**, 147–158 (2008).

[10] Tomschik, M., Zheng, H., van Holde, K., Zlatanova, J., and Leuba, S. Fast, long-range, reversible conformational fluctuations in nucleosomes revealed by single-pair fluorescence resonance energy transfer. *Proc. Natl. Acad. Sci. U.S.A.* **102**, 3278–3283 (2005).

[11] Correction for Tomschik et al. , Fast, long-range, reversible conformational fluctuations in nucleosomes revealed by single-pair fluorescence resonance energy transfer. *Proc. Natl. Acad. Sci. U.S.A.* **105**, 10632–10632 (2008).

[12] Koopmans, W. J. A., Brehm, A., Logie, C., Schmidt, T., and van Noort, J. Single-pair FRET microscopy reveals mononucleosome dynamics. *J. Fluoresc.* **17**, 785–795 (2007).

[13] Li, G., Levitus, M., Bustamante, C., and Widom, J. Rapid spontaneous accesibility of nucleosomal DNA. *Nat. Struct. Mol. Biol.* **12**, 46–53 (2005).

[14] Schiessel, H. The physics of chromatin. *J. Phys.: Condens Matter* **15**, R699–R774 (2003).

[15] Claudet, C., Angelov, D., Bouvet, P., Dimitrov, S., and Bednar, J. Histone octamer instability under single molecule experiment conditions. *J. Biol. Chem.* **280**, 19958–19965 (2005).

[16] Thåström, A., Gottesfeld, J., Luger, K., and Widom, J. Histone - DNA binding free energy cannot be measured in dilution-driven dissociation experiments. *Biochemistry* **43**, 736–741 (2004).

[17] Yager, T., Mcmurray, C., and Vanholde, K. Salt-Induced Release of DNA from Nucleosome Core Particles. *Biochemistry* **28**, 2271–2281 (1989).

[18] Lusser, A. and Kadonaga, J. Strategies for the reconstitution of chromatin. *Nat. Methods* **1**, 19–26 (2004).

[19] Rasnik, I., Mckinney, S., and Ha, T. Surfaces and orientations: Much to FRET about? *Acc. Chem. Res.* **38**, 542–548 (2005).

[20] Zhuang, X., Bartley, L., Babcock, H., Russell, R., Ha, T., Herschlag, D., and Chu, S. A single-molecule study of RNA catalysis and folding. *Science* **288**, 2048–2051 (2000).

[21] Rasnik, I., Myong, S., Cheng, W., Lohman, T., and Ha, T. DNA-binding orientation and domain conformation of the E-coli Rep helicase monomer bound to a partial duplex junction: Single-molecule studies of fluorescently labeled enzymes. *J. Mol. Biol.* **336**, 395–408 (2004).

[22] Boukobza, E., Sonnenfeld, A., and Haran, G. Immobilization in surface-tethered lipid vesicles as a new tool for single biomolecule spectroscopy. *J. Phys. Chem. B* **105**, 12165–12170 (2001).

[23] Dickson, R., Norris, D., Tzeng, Y., and Moerner, W. Three-dimensional imaging of single molecules solvated in pores of poly(acrylamide) gels. *Science* **274**, 966–969 (1996).

[24] Lu, H., Xun, L., and Xie, X. Single-molecule enzymatic dynamics. *Science* **282**, 1877–1882 (1998).

[25] Heyes, C., Kobitski, A., Amirgoulova, E., and Nienhaus, G. Biocompatible surfaces for specific tethering of individual protein molecules. *J. Phys. Chem. B* **108**, 13387–13394 (2004).

[26] Kapanidis, A., Laurence, T., Lee, N., Margeat, E., Kong, X., and Weiss, S. Alternating-laser excitation of single molecules. *Acc. Chem. Res.* **38**, 523–533 (2005).

[27] Amirgoulova, E., Groll, J., Heyes, C., Ameringer, T., Rocker, C., Moller, M., and Nienhaus, G. Biofunctionalized polymer surfaces exhibiting minimal interaction towards immobilized proteins. *ChemPhysChem* **5**, 552–555 (2004).

[28] Lowary, P. and Widom, J. New DNA sequence rules for high affinity binding to histone octamer and sequence-directed nucleosome positioning. *J. Mol. Biol.* **276**, 19–42 (1998).

[29] Chrambach, A. and Rodbard, D. Polyacrylamide gel electrophoresis. *Science* **172**, 440–451 (1971).

[30] Lackowicz, J. *Principles of Fluorescence Spectroscopy*, volume 2nd. Kluwer Academic / Plenum Publishers, New York, (1999).

[31] Dickson, R., Cubitt, A., Tsien, R., and Moerner, W. On/off blinking and switching behaviour of single molecules of green fluorescent protein. *Nature* **388**, 355–358 (1997).

[32] Gai, H., Griess, G., Demeler, B., Weintraub, S., and Serwer, P. Routine fluorescence microscopy of single untethered protein molecules confined to a planar zone. *J. Microsc.* **226**, 256–262 (2007).

[33] Groll, J., Ameringer, T., Spatz, J., and Moeller, M. Ultrathin coatings from isocyanate-terminated star PEG prepolymers: Layer formation and characterization. *Langmuir* **21**, 1991–1999 (2005).

[34] Godde, J. and Wolffe, A. Disruption of Reconstituted Nucleosomes - the Effect of Particle Concentration, $MgCl_2$ and KCl Concentration, the Histone Tails, and Temperature. *J. Biol. Chem.* **270**, 27399–27402 (1995).

[35] Rasnik, I., Mckinney, S., and Ha, T. Nonblinking and longlasting single-molecule fluorescence imaging. *Nat. Methods* **3**, 891–893 (2006).

[36] Cognet, L., Harms, G., Blab, G., Lommerse, P., and Schmidt, T. Simultaneous dual-color and dual-polarization imaging of single molecules. *Appl. Phys. Lett.* **77**, 4052–4054 (2000).